DTI Analysis Methods: Region of Interest Analysis

9

Martijn Froeling, Pim Pullens, and Alexander Leemans

Learning Points

- Different strategies to define regions of interest (ROI)
- Advantages and limitations of a ROI analysis
- Effects of ROI size, co-registration, and statistical analysis methods on results

Introduction

The region of interest (ROI) analysis method is based on the delineation of predefined areas of the image and is a commonly used method for quantitative analysis of diffusion tensor imaging data. A ROI is defined as a selected area of an image from which the individual or average pixel values are extracted for further analysis. The ROI commonly has to be manually drawn, but in some cases it can be obtained by (semi-)automated segmentation. The chosen region can be a geometrical shape (i.e., sphere, cube) or be defined by the shape of the anatomical structure of interest. The first is faster but less precise, whereas the second option is more time consuming but in general gives more accurate results, as will be discussed further on.

Overall the ROI analysis method is relatively easy to use and is supported by most diffusion tensor imaging data analysis software [1]. Its main benefit is the high sensitivity to small changes of the parameters of interest [2]. Additionally the method requires only little technical know-how compared to other techniques discussed later on in this and following chapters. However, it also has numerous drawbacks. ROI analysis is very time consuming and a clear hypotheses about the location of pathology is needed. Therefore it does not allow for full brain coverage and requires at least a moderate knowledge of the anatomy. Furthermore, even with expert knowledge of the anatomy and precise ROI definition the technique is very susceptible to inter- and intra-user variability.

This section covers the basis of ROI analysis, when to use and more importantly when not to use the technique. When applying ROI analysis a clear hypotheses is needed and the ROIs have to be accurately defined. Important considerations

M. Froeling, PhD (✉)
Image Sciences Institute, University Medical Center Utrecht, Heidelberglaan 100, 3584 CX Utrecht, The Netherlands
e-mail: m.froeling@umcutrecht.nl

P. Pullens, PhD
icometrix, Leuven, Belgium

Department of Radiology, Antwerp University Hospital, University of Antwerp, Antwerp, Belgium

A. Leemans, PhD
PROVIDI Lab, Image Sciences Institute, University Medical Center Utrecht, Utrecht, The Netherlands

W. Van Hecke et al. (eds.), *Diffusion Tensor Imaging*, DOI 10.1007/978-1-4939-3118-7_9

that will be discussed are the effect of the position and size, ROI normalization, image registration, and statistical analysis.

When to Use ROI Analysis

Because of its good sensitivity, ROI analysis is best performed when a clear hypothesis is present about the expected differences in white matter in a well-defined region of the brain. As stated in the introduction, the region can be defined by anatomical structure (e.g., corpus callosum, amygdala), pathology (stroke, lesion, tumor, etc.), geometry (sphere, cube, etc.) or input from another modality, e.g., fMRI. The ROI should not be too large in size, because of statistical reasons explained further on in this chapter. ROI analysis is especially useful in regions where there are lesions, e.g., tumors. In these cases tract based analysis (TBA) might be impossible due to the lack of normal fiber pathways. Furthermore, registration of a brain with lesions to a standard brain atlas may be difficult or flawed due to deviations from the normal anatomy.

When Not to Use ROI Analysis

ROI analysis can clearly not been used if there is no hypothesis about the location of the effects in the brain. If structural data are absent or of poor quality, other methods such as extraction of diffusion metrics from fiber bundles, histogram analysis [3, 4], voxel-based analysis [5], or TBSS [6] might be better suited, as will be discussed in the next chapters.

Well-Defined Regions

To define a ROI usually the region is drawn by hand on a structural MRI image (T1/T2 weighted). To the investigator ("anatomist") it should be clear what the borders of the regions are and to what extent it should be included. For example, the corpus callosum could be outlined on a mid-sagittal slice and extended 2–3 slices laterally in both directions.

ROIs can also be defined on FA or ADC images, especially when white matter structures are being investigated, where contrast is minimal on a T1- or T2-weighted image. In this approach care must be taken not to fall into the trap of circular reasoning, because drawing of the ROI is not independent of the studied data. This approach can also be taken when investigating pathologies on ipsi- and contralateral sides of the brain as is shown in the next paragraph.

Some pathologies, stroke for instance, are clearly visible on a trace or ADC map, but not on other modalities, as is shown in Fig. 9.1. In this case the trace or ADC map is the obvious choice for ROI definition. By mirroring the ROI to the contralateral side of the brain, DW metrics can be studied in both affected and healthy tissue.

When the researcher is interested in a sub-part of a certain structure and wants to have control over the size of the ROI, a geometrical ROI (circle/sphere, square/cube, etc.) could be used. The ROI is then placed in the center of the structure and has the same size in each subject, in contrast

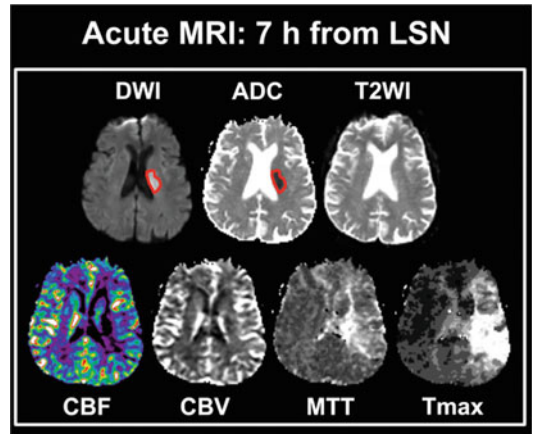

Fig. 9.1 Multimodality data from a stroke patient, 7 h since last seen normal (LSN). Note the difference in contrast between different modalities. In this case, the DWI and ADC maps provide excellent contrast for ROI definition of the stroke area: hyperintense on DWI, hypointense on ADC. *DWI* diffusion-weighted image, *ADC* apparent diffusion coefficient, *T2WI* T2-weighted image, *CBF* cerebral blood flow, *CBV* cerebral blood volume, *MTT* mean transit time, *Tmax* time to max in perfusion [adapted from Wu et al. [7]. With permission from Wolters Kluwer Health]

to manual ROI delineation where ROI size is different for each subject.

The sites of activation of a BOLD fMRI study can also serve as a ROI, for example to start tractography, and it may lead to a very-well-localized ROI in each subject. Because the main signal is in the gray matter, it may be necessary to dilate the ROI into the white matter [8–10].

Atlas-Based ROIs

There are multiple predefined atlases of white matter available, and these may serve as good starting points for ROI analysis. Well-known atlases are the JHU atlas [11] and the probabilistic Juelich atlas [12]. Data from multiple subjects is used to create a 3-D overview of well-defined brain regions. A key advantage of using an atlas is that it is created in a standard space (i.e., MNI, Talaraich), which makes it easy to compare between subjects or studies. A common approach is therefore to register the subject's data to the atlas data, or vice versa. When using atlases, care must be taken to check overlap of the regions with the data under study, as misalignment may obscure region location. Once the data is correctly aligned, diffusion measures such as FA or ADC can be easily extracted from predefined regions such as corpus callosum, fornix etc.

ROI Definition

While relatively easy to implement, there are some important things to keep in mind when performing ROI analysis. As mentioned before, a ROI can be best defined on high quality T1 or T2 weighted anatomical reference images. This is to avoid bias of defining the ROI on the parameter map of interest, which may influence the position and boundaries or the ROI. However, when choosing this approach one has to take great care that the ROI position on the reference images and the parameter map of interest are aligned as illustrated in Fig. 9.2. In this figure the contour of the brain derived from the reference scan is overlaid on the diffusion weighted images and the FA map. Both images were acquired during the same scanning session, which should assure

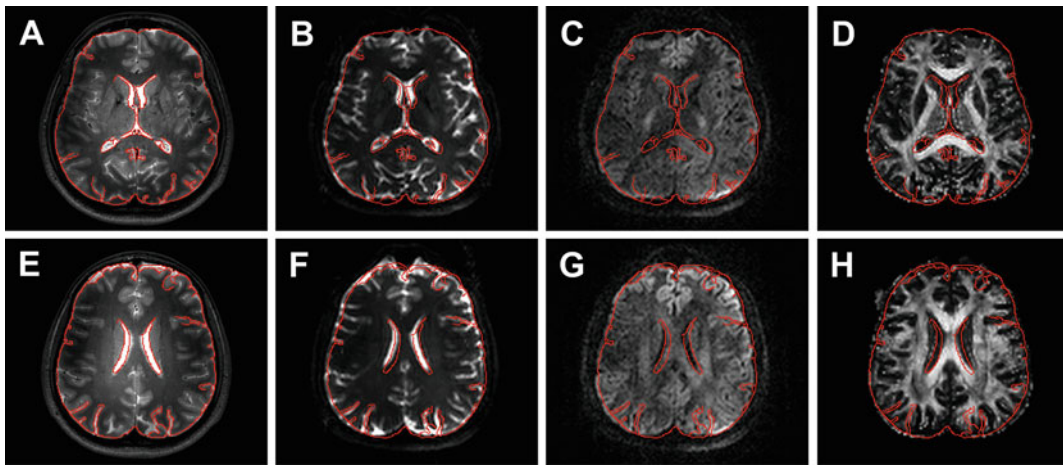

Fig. 9.2 Examples of misalignment between different image types. *Panels* (**a**) and (**e**) show high-resolution T2-weighted images with the contour of the brain outlined in *red*. This contour is overlaid on the corresponding unweighted ($b=0$, (**b**) and (**f**)) and diffusion weighted ($b=1000$ s/mm^2, (**c**) and (**g**)) images and the FA map (**d** and **h**)

a good alignment. At first sight, the un-weighted and the diffusion-weighted images seem to match well with the reference image. However, closer examination clearly shows misalignment. This same misalignment may not be so apparent when just looking at the corresponding FA map (see Fig. 9.2d, h).

The origin of the discrepancy between the different images can have multiple reasons but can have a great effect on parameter quantification and fiber tractography [13]. One common reason for misalignment is that the diffusion images are usually acquired with a single-shot EPI readout, which commonly has nonrigid geometric distortions due to its sensitivity to susceptibility artifacts (see Chap. 6). Furthermore, there can be patient motion in between acquisition of the reference image and diffusion data within the same scan protocol. This motion causes rigid misalignment of the images

Effect of Motion and Size

Although the distortions and offset might seem negligible, one has to realize that only a small misalignment can have serious impact on the parameter estimation. To illustrate this point, two regions of interest in the corpus callosum were defined. Both the regions were based on the anatomical reference image as well as the FA map (see Fig. 9.3). Furthermore, the size of the two different ROIs was varied to illustrate the effect of partial volume effects and user bias in defining the regions of interest. The results for the average FA and MD values from these different ROIs are given in Table 9.1. The variation of the parameters clearly emphasizes the sensitivity of the technique to ROI definition and positioning [14]. Small ROIs will typically be more sensitive to erroneous voxels within the ROI. Increasing the ROI size will generally decrease the sensitivity to these errors, but will increase contamination by other structures, also known as partial volume effects, decreasing the sensitivity [15].

This implies that the definition of the ROIs should be done with great care and accuracy. Although the positioning of circles or rectangles is fast and easy it is generally better to accurately outline the ROI according to the shape of the structure. The latter is more time consuming but can greatly help minimize the inclusion of other structures [16]. Another way to exclude different types of tissue is to exclude pixels based on diffusion parameters. For example one can exclude cerebrospinal fluid by excluding pixels with high

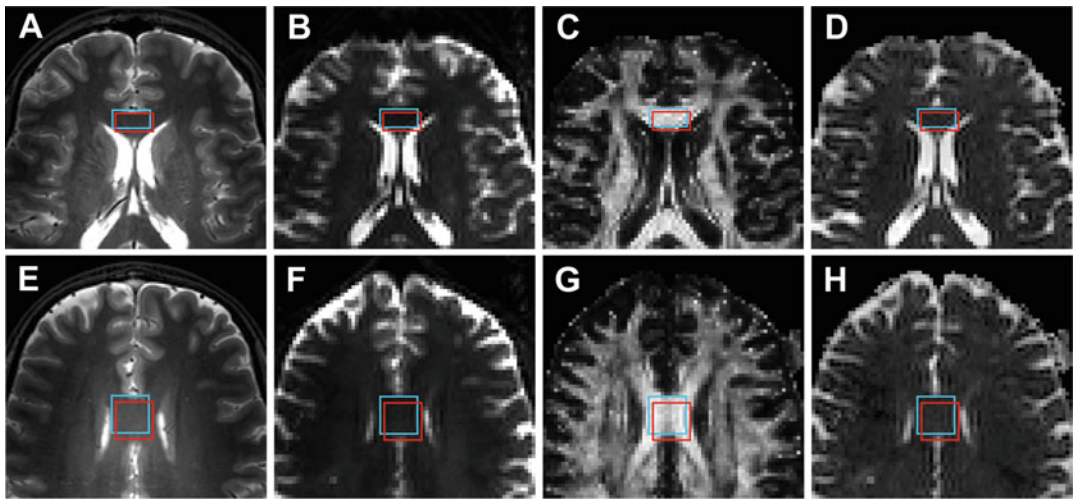

Fig. 9.3 Two examples of a rectangular ROI selecting the frontal and middle part of the corpus callosum. For each region one ROI was drawn based on the high-resolution reference scan (*red*) and one ROI was drawn based on the FA map (*blue*). The selections are shown on the T2-weighted anatomical image (**a** and **e**), the un-weighted diffusion image (**b** and **f**), the FA map (**c** and **g**), and the MD map (**d** and **h**)

Table 9.1 Average values for two part of the corpus callosum for different sizes of manually drawn rectangular regions of interest. The ROIs were drawn both on the anatomical reference images and the FA maps

		Anatomy		FA map	
	Size (pixels)	FA	MD ($\times 10^{-3}$ mm^2/s)	FA	MD ($\times 10^{-3}$ mm^2/s)
Front	3×5	0.71±0.20	0.82±0.44	0.81±0.11	0.77±0.17
	5×7	0.59±0.33	1.19±0.82	0.77±0.20	0.85±0.49
	7×9	0.52±0.35	1.34±0.87	0.63±0.28	0.96±0.58
Mid	7×7	0.75±0.13	0.79±0.11	0.80±0.10	0.76±0.13
	9×9	0.75±0.16	0.80±0.17	0.75±0.16	0.85±0.32
	11×11	0.75±0.19	0.81±0.23	0.71±0.22	0.93±0.47

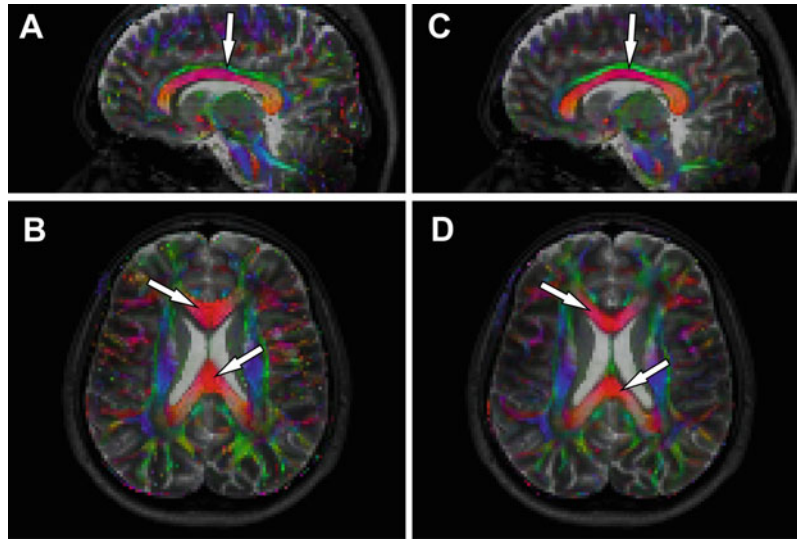

Fig. 9.4 Color coded FA maps overlaid on high resolution anatomical images to illustrate the result of non-rigid registration for EPI distortion correction. The images on the *left* (**a** and **b**) show the uncorrected data, whereas the images on the *right* (**c** and **d**) show the corrected data. The *white arrows* indicate locations where the correction of the misalignment is clearly visible

MD and low FA. However, with this method it is also possible to exclude the tissue of interest with pathology and thus affected parameters.

Registration

There are multiple strategies to correct for the distortions of the EPI images, e.g., B0 field mapping [17, 18], point spread function mapping [19, 20], or reversed gradient acquisition [21, 22]. However, these correction methods demand an extra data acquisition prolonging scan time. Another commonly available method is image registration (see Chap. 10). This technique is widely available in data processing software [1]. Figure 9.4 shows an example of nonrigid registration to correct for the misalignment between the diffusion tensor imaging data and the corresponding anatomical reference data. In panel A and B one can clearly see the misalignment between the corpus callosum, shown in red on the color-coded FA map, and the lateral ventricles, shown in white on the anatomical reference image. After nonrigid registration using *ExploreDTI* [23] one can appreciate the correct alignment of these structures as shown in panel C

Table 9.2 Average values for two part of the corpus callosum based on three manually drawn regions of interest in the corpus callosum based on T1 images before and after registration

	Normal		Corrected	
	FA	MD ($\times 10^{-3}$ mm^2/s)	FA	MD ($\times 10^{-3}$ mm^2/s)
ROI1	0.70±0.20	0.82±0.33	0.76±0.14	0.77±0.14
ROI2	0.70±0.18	0.81±0.24	0.78±0.12	0.76±0.14
ROI3	0.67±0.23	0.95±0.38	0.70±0.20	0.95±0.34

and D. The effect of registration on parameters estimated from ROIs drawn on the anatomical image are shown in Table 9.2. The ROIs were drawn in the regions indicated by the white arrows. In this example the FA increases and MD decreases after registration. For all parameters the standard deviation decreased.

Spatial Normalization

Spatial normalization is the process of bringing the study data into a common stereotaxic space. It is a crucial step for group analysis of MRI data and it allows for use of a standard 3D coordinate space for analysis and reporting of neuroimaging data [24]. It consists of mapping the individual subject data to a template, for instance to the well-known Talairach brain [25] or the MNI template [26]. Once the data is in common space, ROIs can be easily compared and checked for accuracy in size and location. An example is shown in Fig. 9.5. It is recommended not to transfer tensor data into a common space, because interpolation of tensor data is not straightforward and data will be corrupted [28]. Consequently, one should only use scalar maps (FA, ADC, etc.) for conversion into a standard space.

Statistical Analysis

The choice of which statistical method to use depends on the hypotheses and experimental set up [29]. When there is a clear hypothesis and a corresponding well-defined anatomical region, the ROI analysis can be very sensitive. However, when the hypothesis is less strong and multiple regions are investigated, a correction for multiple comparisons should be carried out to reduce false positives [30]. More specifically, when there is no effect of the null hypothesis, and a p-value of 0.05 is used, 5 out of each of 100 comparisons will falsely reject the null hypothesis (known as alpha error or type 1 error). There are numerous possibilities to correct for the multiple comparison problem. One of the most commonly used but also the most conservative is the Bonferroni correction, which treats each comparison as an independent experiment. This implies that the p-value at which the null hypothesis is rejected has to be divided by the number of comparisons. So for ten different ROIs the p-value will be 0.005 instead of 0.05, i.e., 0.05/10. The p-value becomes even lower when multiple parameters are compared. If FA and MD are evaluated in these ten regions, the Bonferroni threshold of significance will even decrease to 0.0025, i.e., 0.05/20.

As stated before, ROI analysis is highly user dependent as variability in ROI placement is easily introduced by different observers. Secondly, variability might be introduced when multiple datasets from the same subject are analyzed by a single observer at different time points. It is therefore good practice to calculate inter- and intra-observer agreement (for instance, using the κ-statistic) [31]. Agreement can be calculated on the basis of extracted DTI metrics (FA, ADC) but also, as percent overlap, on the actual ROI coordinates. The demonstrated overlap in Fig. 9.5 for multiple subjects should then be replaced by the inter- or intra-observer overlap.

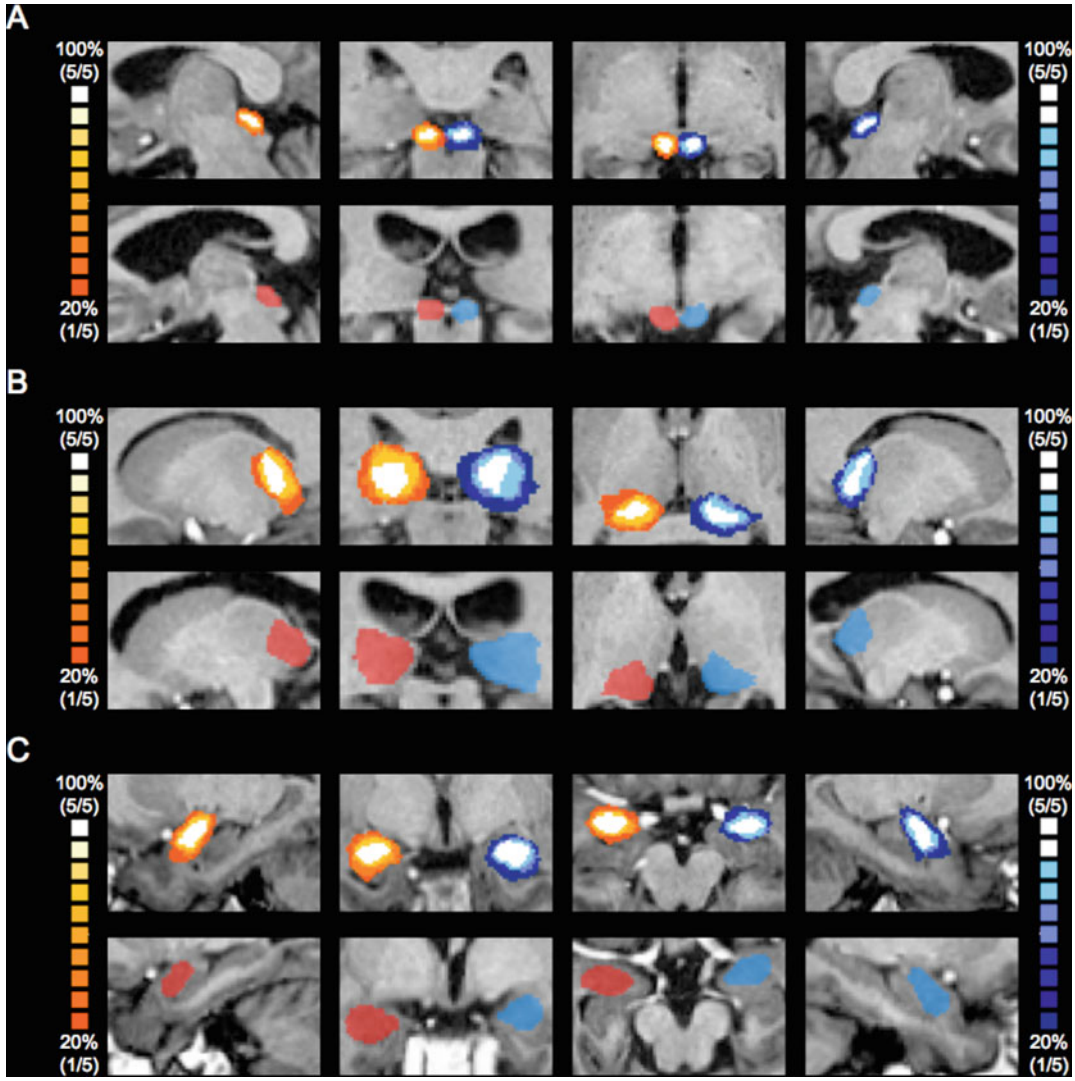

Fig. 9.5 An example of ROI overlap in ten healthy controls (*top rows* in each *panel* **a**–**c**) and patient (*bottom rows*). The ROIs were drawn in native space first, and then mapped into Talairach space and combined to form probabilistic maps of ROI overlap [adapted from Tamietto et al. [27]. With permission from Elsevier]

Summary: The Pros and Cons of ROI Analysis

In conclusion, ROI analysis is a simple and effective means to investigate white matter changes in small, well defined regions on good quality data. However, the technique is prone to error and not suitable for the investigation of structures with complex boundaries or poorly defined changes in white matter microstructure. This particularly applies for areas of compromised data quality. The delineation of ROIs can be very time consuming and both intra and inter-rater measures are poorly reproducible which impacts on both cross-sectional and longitudinal studies [32–34]. Furthermore, ROI placement without any prior knowledge can lead to inaccurate ROI segmentation which will result in different degrees of partial voluming. Therefore ROI analysis is highly user dependent and reliability measures need to be calculated to assess the quality of the results.

References

1. Soares JM, Marques P, et al. A hitchhiker's guide to diffusion tensor imaging. Front Neurosci. 2013;7:31.
2. Cercignani M. Strategies for patient–control comparison of diffusion MR data. In: Jones DK, editor. Diffusion MRI theory, methods, and applications. New York, NY: Oxford University Press; 2011.
3. Law M, Young R, et al. Histogram analysis versus region of interest analysis of dynamic susceptibility contrast perfusion MR imaging data in the grading of cerebral gliomas. AJNR Am J Neuroradiol. 2007;28(4):761–6.
4. Young R, Babb J, et al. Comparison of region-of-interest analysis with three different histogram analysis methods in the determination of perfusion metrics in patients with brain gliomas. J Magn Reson Imaging. 2007;26(4):1053–63.
5. Snook L, Plewes C, et al. Voxel based versus region of interest analysis in diffusion tensor imaging of neurodevelopment. Neuroimage. 2007;34(1): 243–52.
6. Smith SM, Jenkinson M, et al. Tract-based spatial statistics: voxelwise analysis of multi-subject diffusion data. Neuroimage. 2006;31(4):1487–505.
7. Wu O, Dijkhuizen RM, et al. Multiparametric magnetic resonance imaging of brain disorders. Top Magn Reson Imaging. 2010;21(2):129–38.
8. Kleiser R, Staempfli P, et al. Impact of fMRI-guided advanced DTI fiber tracking techniques on their clinical applications in patients with brain tumors. Neuroradiology. 2010;52(1):37–46.
9. Mazerolle EL, Beyea SD, et al. Confirming white matter fMRI activation in the corpus callosum: co-localization with DTI tractography. Neuroimage. 2010;50(2):616–21.
10. Preti MG, Makris N, et al. A novel approach of fMRI-guided tractography analysis within a group: construction of an fMRI-guided tractographic atlas. Conf Proc IEEE Eng Med Biol Soc. 2010;2012:2283–6.
11. Oishi K, Zilles K, et al. Human brain white matter atlas: identification and assignment of common anatomical structures in superficial white matter. Neuroimage. 2008;43(3):447–57.
12. Eickhoff SB, Stephan KE, et al. A new SPM toolbox for combining probabilistic cytoarchitectonic maps and functional imaging data. Neuroimage. 2005;25(4): 1325–35.
13. Irfanoglu MO, Walker L, et al. Effects of image distortions originating from susceptibility variations and concomitant fields on diffusion MRI tractography results. Neuroimage. 2012;61(1):275–88.
14. Pajevic S, Basser PJ. Parametric and non-parametric statistical analysis of DT-MRI data. J Magn Reson. 2003;161(1):1–14.
15. Vos SB, Jones DK, et al. Partial volume effect as a hidden covariate in DTI analyses. Neuroimage. 2011;55(4):1566–76.
16. Jones DK, Cercignani M. Twenty-five pitfalls in the analysis of diffusion MRI data. NMR Biomed. 2010;23(7):803–20.
17. Chen NK, Wyrwicz AM. Correction for EPI distortions using multi-echo gradient-echo imaging. Magn Reson Med. 1999;41(6):1206–13.
18. Jezzard P, Balaban RS. Correction for geometric distortion in echo planar images from B0 field variations. Magn Reson Med. 1995;34(1):65–73.
19. Robson MD, Gore JC, et al. Measurement of the point spread function in MRI using constant time imaging. Magn Reson Med. 1997;38(5):733–40.
20. Zeng H, Constable RT. Image distortion correction in EPI: comparison of field mapping with point spread function mapping. Magn Reson Med. 2002;48(1): 137–46.
21. Andersson JL, Skare S. A model-based method for retrospective correction of geometric distortions in diffusion-weighted EPI. Neuroimage. 2002;16(1):177–99.
22. Chang H, Fitzpatrick JM. A technique for accurate magnetic resonance imaging in the presence of field inhomogeneities. IEEE Trans Med Imaging. 1992;11(3):319–29.
23. Leemans A, Jeurissen B, et al. ExploreDTI: a graphical toolbox for processing, analyzing, and visualizing diffusion MR data. Proceedings 17th Scientific Meeting, International Society for Magnetic Resonance in Medicine, Honolulu; 2009.
24. Evans AC, Janke AL, et al. Brain templates and atlases. Neuroimage. 2012;62(2):911–22.
25. Talairach J, Tournoux P. Co-planar stereotaxic atlas of the human brain: 3-dimensional proportional system - an approach to cerebral imaging. New York, NY: Thieme Medical Publishers; 1988.
26. Evans AC, Collins DL, et al. 3D statistical neuroanatomical models from 305 MRI volumes. Nuclear Science Symposium and Medical Imaging Conference, 1993. 1993 IEEE Conference Record; 1993.
27. Tamietto M, Pullens P, et al. Subcortical connections to human amygdala and changes following destruction of the visual cortex. Curr Biol. 2012;22(15): 1449–55.
28. Arsigny V, Fillard P, et al. Log-Euclidean metrics for fast and simple calculus on diffusion tensors. Magn Reson Med. 2006;56(2):411–21.
29. Dupont WD, editor. Statistical modeling for biomedical researchers. Cambridge: Cambridge University Press; 2009.
30. Miller RG, editor. Simultaneous statistical inference. New York, NY: Springer; 1981.
31. Ozturk A, Sasson AD, et al. Regional differences in diffusion tensor imaging measurements: assessment of intrarater and interrater variability. AJNR Am J Neuroradiol. 2008;29(6):1124–7.
32. Astrakas LG, Argyropoulou MI. Shifting from region of interest (ROI) to voxel-based analysis in human brain mapping. Pediatr Radiol. 2010;40(12): 1857–67.
33. Chanraud S, Zahr N, et al. MR diffusion tensor imaging: a window into white matter integrity of the working brain. Neuropsychol Rev. 2010;20(2):209–25.
34. Mukherjee P, Chung SW, et al. Diffusion tensor MR imaging and fiber tractography: technical considerations. AJNR Am J Neuroradiol. 2008;29(5):843–52.